

# The Intergalactic Medium and the Energy Distribution of Quasars

Luc Binette, Mario Rodríguez-Martínez and Isidro Ballinas

*Instituto de Astronomía, Universidad Nacional Autónoma de México,  
Apartado Postal 70-264, 04510 México, DF, Mexico*

**Abstract.** The ionizing spectral energy distribution of quasars is known to exhibit a steepening of the distribution short-ward of  $1050\text{\AA}$ . It has been assumed that this change of power-law index from  $-1$  to  $-2$  is intrinsic to the quasars. We study an alternative interpretation, in which a tenuous absorption screen is responsible for the change of index. A successful spectral fit is obtained using a total hydrogen density distribution decreasing with redshift as  $\sim (1+z)^\xi$  with  $\xi$  of the order  $-3.5$  if we suppose that the ionization state of the intervening gas is controlled by the line-of-sight quasar. This interpretation is not compatible, however, with the relative weakness of the observed quasar intensities with respect to that of the local background metagalactic radiation. Therefore, our interpretation in its present form cannot be sustained.

## 1. Introduction

The ionizing spectral energy distribution (hereafter ISED) of nearby active galactic nuclei cannot be observed directly due to the galactic absorption beyond the Lyman limit. Owing to the redshift effect, however, we can get a glimpse of the ISED from the spectra of very distant quasars. Most studies on the subject indicate a steepening of the distribution at wavelengths shorter than  $1000\text{\AA}$  (see O'Brien et al. 1988) and references therein). The most extensive work on the subject has been performed by Zheng et al. (1997, ZKTGD) using HST archived data. They found that the power-law index ( $F_\nu \propto \nu^\alpha$ ) steepens from  $\approx -1$  for  $\lambda > 1050\text{\AA}$  to  $\approx -2$  for shorter wavelengths.

Korista, Ferland & Baldwin (1997) pointed out that such a steep slope for the ISED would imply an insufficient number of photons beyond  $h\nu > 54.4\text{ eV}$  to account for the observed luminosities of the high excitation emission lines.

We report preliminary results of our attempt to find an alternative explanation for the break, one that is *extrinsic* to the quasar ISEDs. We postulate the existence of a very tenuous absorption gas component pervading the local universe and proceed to study the characteristics it must possess to reproduce the observed break, and its place and role within our IGM views.

## 2. Data simulation to a first order

The composite spectrum of ZKTGD was constructed by merging 284 spectra of 101 quasars taken with FOS of the Hubble telescope. Although the wavelength coverage of individual spectra was relatively narrow, the distribution in quasar redshifts allowed ZKTGD to cover the wavelength range of 310–3000 Å in the quasar rest-frame. Before merging their spectra, each spectrum was corrected for the Lyman valley and Ly $\alpha$  forest absorption by calculating the appropriate transmission curve using the scheme developed by Møller & Jakobsen (1990).

Our aim is to reproduce the change of ISED index by introducing a previously unknown intergalactic absorption component. This component must consist of clumps which are sufficiently optically thin (and numerous) that they do not show up as individually detectable Ly $\alpha$  absorption lines in the archived FOS spectra, hence  $N_{H^0} \ll 10^{12} \text{ cm}^{-2}$ . In this preliminary work, we did not fully simulate the observed data on a pixel by pixel basis, rather we defined a single spectrograph wavelength window (3000 Å to 1300 Å) which we considered typical of the wavelength coverage of individual quasars and then redshifted this window in locked steps. We defined a *source* array,  $F_j$ , to represent the intrinsic SED of all quasars. This SED consisted of a power-law of index  $\alpha$ . All arrays were evenly binned in  $\text{Log}\lambda$  and the wavelength of each array element  $j$  was such that  $\text{Log}\lambda_j = \text{Log}\lambda_{MAX} - j \times u$ , with  $u = \text{Log}(1 + \delta z_o)$  and  $\lambda_{MAX}$  being the highest rest-wavelength considered. The advantage of this scheme is that the source array  $F_j$  can be redshifted by simple translation of the pointers  $j$  provided the redshift is a multiple of  $\delta z_o$ . This is not a serious limitation if one chooses a sufficiently small  $\delta z_o$  (we used 0.01). The procedure followed consisted in translating the source array by an integer number of bins  $k$  and then add it to our averaging buffer:  $B_j = B_j + w_k F_j T_j(z_Q^k, \lambda_j)$  where  $T_j$  is the transmission function evaluated at  $\lambda_j$  for the  $k^{\text{th}}$  array spectrum (corresponding to a quasar's redshift  $z_Q^k = k \delta z_o$ ), and  $w_k$  is the global weight given to the  $k^{\text{th}}$  array before summing. These ‘uniform’ weights were based on the dispersion vs. rest-frame wavelength relation displayed in the Fig. 6 of ZKTGD. More specifically,  $w_k = s_k^{-2}$  where  $s_k = \bar{\lambda}_{kc}^{-0.71}$  with  $\bar{\lambda}_{kc} = 2150(1 + z_Q^k) \text{ Å}$ , the central wavelength of redshifted array  $k$ . The lowest and highest redshifts considered were 0.33 and 3.5, respectively, which are the values quoted by ZKTGD for their data set. We uniformly covered this redshift interval by considering all integer values of  $k$  between these two redshift limits.

## 3. The transmission function

For each quasar rest-frame wavelength bin  $j$ , we calculated the transmitted intensity  $I_{\lambda_j}^{tr} = I_{\lambda_j} T_{\lambda_j} = I_{\lambda_j} e^{-\tau(\lambda_j)}$  by integrating the opacity along the line-of-sight to a quasar of redshift  $z_Q$

$$\tau(\lambda_j) = \sum_{i=0}^{10} \int_0^{z_Q} \sigma_i \left( \frac{\lambda_j}{1+z} \right) n_{H^0}(z) \frac{dl}{dz} dz \quad (1)$$

where  $\lambda_j$  is the quasar rest-frame wavelength for bin  $j$  and  $n_{H^0}(z)$  the intergalactic neutral hydrogen density. The summation was carried out over the different opacity sources: photoionization ( $i = 0$ ) and line absorption from the

Lyman series of hydrogen ( $1 \leq i \leq 10$ ). Although our code could include up to 40 levels, we found that considering only the 10 lowest proved to be adequate. We adopted a fiducial velocity dispersion  $b$  of 30 km/s and assumed a simple line Gaussian profile for  $\sigma_i$  of the lines. Apart from the uniform density absorption case, we also implemented the treatment of a clumpy medium (described later) which was used to ensure that we could reproduce the transmission curve of Møller & Jakobsen (1990) or ZKTGD using parameters appropriate to the Ly $\alpha$  forest. The self imposed constraint that  $N_{H^0} \ll 10^{12} \text{ cm}^{-2}$  for the clumps ensures that we remain in the linear regime of the curve of growth. Therefore, using a uniformly distributed gas or a clumpy medium will be equivalent. The use initially of an homogeneously distributed gas will save us from having to characterize the clumpiness using poorly defined parameters.

For the dependence of the total gas density on redshift, let us consider a simple power-law  $n_H \propto (1+z)^\delta$ . What is lacking is the neutral fraction of  $n_H$  which we will assume to be small and set by equilibrium between photoionization and recombination. In that case, we expect  $n_{H^0}$  to scale proportionally to the (total) density square, and inversely proportionally to the ambient ionizing radiation. We will consider negligible the cumulative opacity of the absorber (as confirmed a posteriori). With those considerations in mind, we obtain that  $n_{H^0}$  should scale as follows with  $z$ :

$$n_{H^0}(z) = n_{H^0}^0 (1+z)^{2(\xi+3)} \Gamma^{-1}(z) (1+\omega)^{-1} \quad (2)$$

where the superscript 0 throughout the text denotes quantities evaluated at  $z = 0$ . In the above expression, we take into account the increase of density with the cosmological scale factor:  $n_H/n_H^0 \propto (1+z)^3$ . The photoionization rate coefficient  $\Gamma$  due to the metagalactic ionizing radiation was parameterized as follows

$$\Gamma(z) = (1+z)^{0.73} e^{-0.526((z-2.3)^2 - 2.3^2)} \quad (3)$$

This is a renormalized version of the parametric fit of Haardt & Madau (1996) who modeled the metagalactic ionizing radiation ( $J_{\nu_0}^{BCK}$ ) taking into account the population evolution of quasars and their luminosity with redshift as well as self-emission of the clumpy intergalactic ionized medium. Note that  $\Gamma(z=0) = 1$  because of our renormalization.

The factor  $(1+\omega)^{-1}$  in equation 2 is the same as that defined by Bajtlik, Duncan & Ostriker (1988) and represents a decrease in the neutral fraction of hydrogen towards the line-of-sight quasar as a result of the ionizing radiation from the quasar. In this expression, the ‘‘proximity’’ term  $\omega$  represents the geometrical dilution of the line-of-sight quasar ionizing flux with respect to the background ionizing radiation:

$$\omega = \left( \frac{r_{1/2}}{r_L} \right)^2 \quad (4)$$

where  $r_L$  is the luminosity distance of the quasar from a parcel of gas at  $z$ .  $r_{1/2}$  if one of our free parameters and correspond to the distance from the quasar where its mean intensity at  $\nu_0$  equals that of the background radiation  $J_{\nu_0}^{BCK}$ . At such distance, the neutral fraction  $x = n_{H^0}/n_H$  is halved due to the quasar

flux.  $r_{1/2}$  can be expressed as follows

$$r_{1/2} = r_{1/2}^0 \sqrt{(1 + z'_Q)^{\alpha-1} \Gamma^{-1}(z)} \quad (5)$$

with

$$r_{1/2}^0 = \frac{1}{4\pi} \sqrt{\frac{L_{\nu_0}^Q}{J_{\nu_0}^{BCK,0}}} \quad (6)$$

where  $\alpha$  is the power-law index of the quasar spectral luminosity distribution ( $L_\nu^Q \propto \nu^\alpha$ ) and  $\nu_0$  is the hydrogen photoionization threshold frequency. As ISED index, we adopt  $\alpha = -0.86$  which is the average index for the radio-quiet subsample of ZKTGD (above 1050Å). In our data simulation, to describe the behavior of  $n_{H0}$  with redshift, we employ only two free parameters:  $\xi$  and  $r_{1/2}^0$ .

In equation 5, the quasar redshift as seen from the absorbing gas at  $z$  is  $z'_Q = (1 + z_Q)/(1 + z) - 1$  while the Hubble constant is  $H' = H_0 \sqrt{\Omega_\Lambda + \Omega_M(1 + z)^3}$  for a flat universe. We assumed the popular  $\Lambda$ CDM universe with  $\Omega_\Lambda = 0.7$  and  $\Omega_M = 0.3$ . To compute the quasar luminosity distance  $r_L(z'_Q)$ , we used the parametric fit of Pen (1999). The light travel distance used to derive  $dl/dz$  was obtained by integration of the Friedmann equation. The adopted value for the Hubble constant is  $H_0 = 67$  km/s/Mpc.

#### 4. Results

Producing a break near 1050 Å followed by a steepened power-law of index  $\sim -2$  is fairly easy to achieve if one disregards any evolution of the background radiation (achieved by setting  $\Gamma = 1$  in Eqn. 2) and adopt the parameters  $\xi = -3.5$ ,  $r_{1/2}^0 = 3200$  Mpc and  $n_{H_0}^0 = 1.9 \times 10^{-11}$  cm $^{-2}$ . This zeroth order model is illustrated by the short-dashed line in Fig. 1 (Model I) and is found to be relatively successful in producing a flat soft ISED. We should point out that photoionization by the line-of-sight quasar, as represented by the parameter  $r_{1/2}^0$ , is an essential ingredient to any successful fit. Actually, if we remove the  $\omega$  term, we consistently obtain a sharp discontinuity at Ly $\alpha$ , as illustrated by the short-dashed dotted line of Model II in Fig. 1. Including line-of-sight quasar photoionization smooths out completely the discontinuity provided  $r_{1/2}^0$  is sufficiently large.

Model I presents, however, the following deficiency. We have compelling evidence that the background radiation increases strongly with  $z$  (c.f. Shull et al. 1999; Davé & Tripp 2001) and references therein. For this reason, varying  $\Gamma(z)$  in equation 2 using the function proposed by Haardt & Madau (1996) is preferable and certainly justified. Models III–VI are such models which span the range  $-5$  to  $-2$  in  $\xi$ . In these models, the parameters  $n_{H_0}^0$  and  $r_{1/2}^0$  were varied in such a way that the different curves superposed as much as possible one another within the interval 500–1000 Å. All of our model parameters are listed in Table 1. We consider Model IV (solid line) to be the one providing the best overall fit. Notice that a broad hump near 500 Å is apparent in all four models which consider  $J_{\nu_0}^{BCK}$  evolution. The hump is only present in the case of the ISED derived from the *radio-quiet* subsample, which is the one plotted in

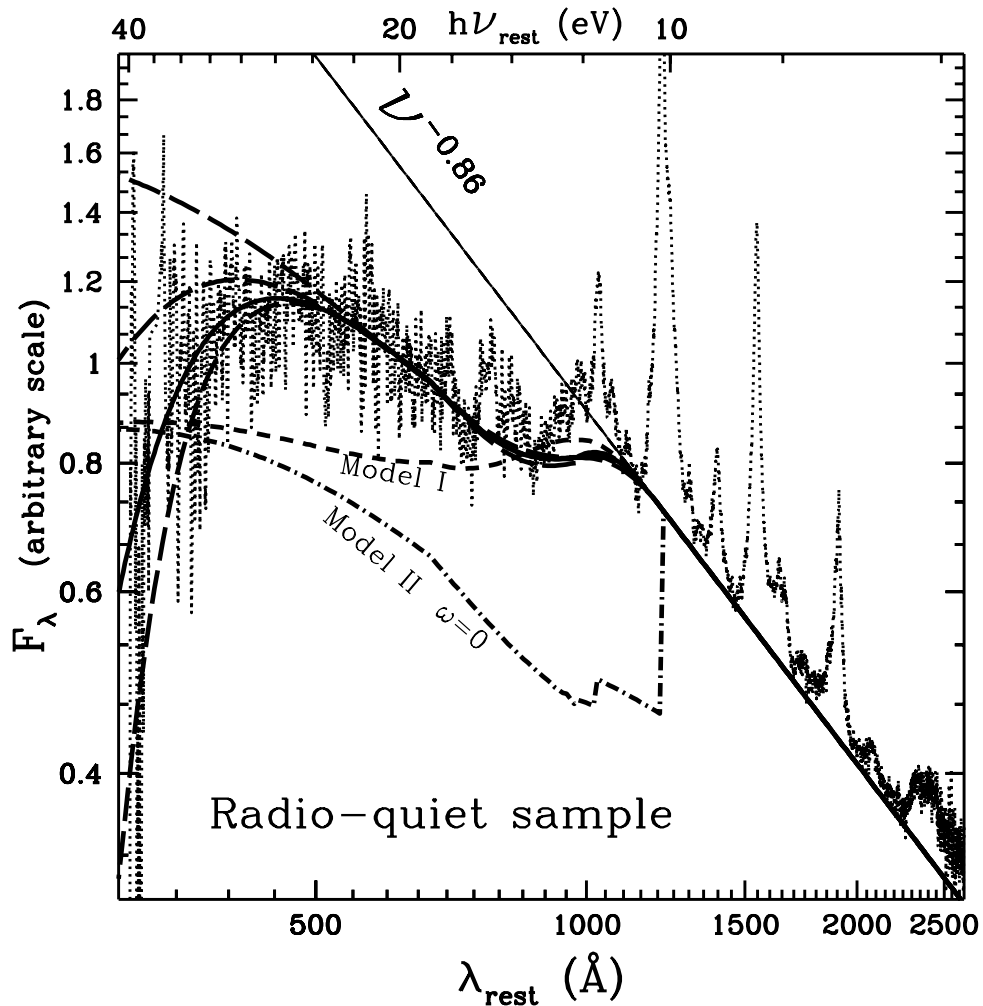


Figure 1. The composite spectrum of radio-quiet quasars constructed by Zheng et al. (1997) (dotted line). The straight short-dashed line represents a power-law fit ( $\alpha = -0.86$ ) above  $1050\text{\AA}$  to the composite continuum underlying the emission lines. The solid line is our favored Model IV ( $\xi = -4$ , see Table 1). Three other models using different values of  $\xi$  are represented by the long-dashed lines. From the top to the bottom curve,  $\xi$  is decreasing from  $-2$  to  $-5$ . The horizontal short-dashed line is Model I which does *not* include redshift evolution of the background radiation. Removing from Model I photoionization by line-of-sight quasar leads to Model II which is represented by the short-dashed dotted line.

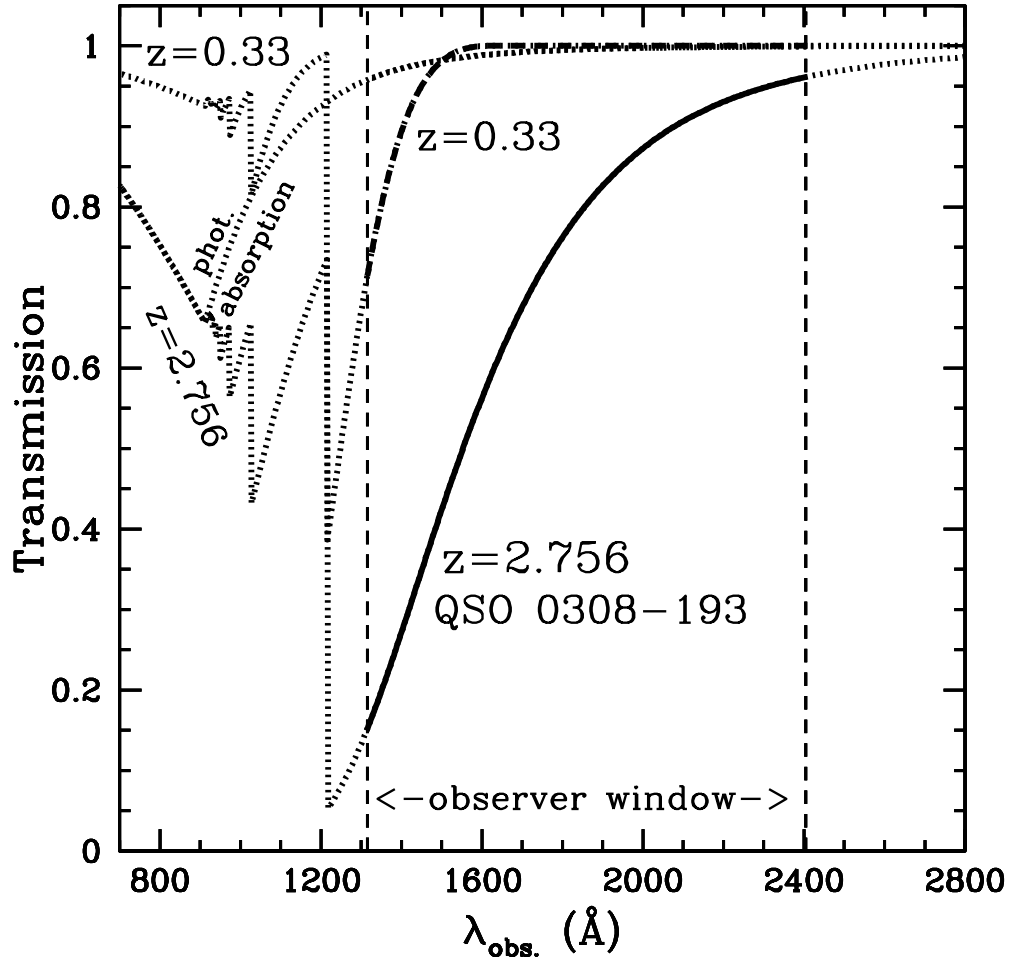


Figure 2. The transmission curve as a function of observed wavelength for our best fit Model IV in the case of the quasar 0308–193 at  $z = 2.756$  (solid line). Outside the FOS spectral window (1315–2400Å), the dotted line shows the continuation of the calculated transmission curve. Starting from the right, the first, second and third descending ramps are contributed in large part by the opacity of Ly $\alpha$ , Ly $\beta$  and Ly $\gamma$  lines, respectively. The small contribution of photoionization to the opacity is shown by the dotted line labeled *phot. absorption*. The short-dashed line represents the transmission curve for the case of a lower redshift quasar at  $z = 0.33$ .

Table 1. Model parameters

Model (ID)	$n_{H^0}^0$ ( $cm^{-3}$ )	$r_{1/2}^0$ (Mpc)	$\xi$ –	$\Gamma$ evol. (Yes/No)
I	$1.9 \times 10^{-11}$	3200	–3.5	N
II	$1.9 \times 10^{-11}$	0	–3.5	N
III	$7.4 \times 10^{-11}$	3200	–5.0	Y
IV	$4.3 \times 10^{-11}$	3200	–4.0	Y
V	$3.2 \times 10^{-11}$	3000	–3.0	Y
VI	$2.4 \times 10^{-11}$	2900	–2.0	Y

Fig. 1. This hump is more apparent than in the ZKTGD paper because of our slightly lower wavelength limit at the UV end. To ascertain the reality of the hump would require a more extensive sample than the current.

## 5. discussion

In appearance successful, our alternative explanation of the steepening of the mean quasar ISED cannot be sustained for the following reasons:

- **A** – In our calculations, we have treated  $r_{1/2}^0$  as a free parameter. Therefore, although we adopted a valid prescription for the variation of the background with  $z$  (eq. 3), we have not considered the issue of the absolute intensity of the background with respect to the observed quasar intensities. It is straightforward to estimate  $\omega = (F_\nu/4\pi J_{\nu_0}^{BCK})^2$  at  $z = 0$  if we adopt an observed quasar flux of  $F_{\lambda_0}^{Q,0} \sim 2 \times 10^{-14} \text{ erg cm}^{-2} \text{ s}^{-1}$  near  $1000 \text{ \AA}$ , which is typical of the quasar sample of ZKTGD. The ionization rate coefficient of Haardt & Madau (1996) of  $4 \times 10^{-14} \text{ s}^{-1}$  at  $z = 0$  translates into a mean intensity of  $J_{\nu_0}^{BCK,0} \approx 1.3 \times 10^{-23} \text{ erg s}^{-1} \text{ sterad}^{-1} \text{ cm}^{-2} \text{ Hz}^{-1}$ , hence  $\omega \approx 5.5 \times 10^{-27} / 1.6 \times 10^{-22} = 3.3 \times 10^{-5}$  (using  $F_{\nu_0} = 912^2 \times 3.3 \times 10^{-19} F_{\lambda_0}$ ). This contradicts our requirement that the proximity effect must extend up to  $z = 0$  for all quasars whose distance is less than 3 Gpc (the approximate value of  $r_{1/2}^0$ ). This estimate of the local value of  $\omega$  clearly shows that the background mean intensity at low  $z$  is much stronger than that of the quasar flux reaching us. Another way of illustrating this is to compare our values of  $r_{1/2}$  with the high redshift value empirically determined of  $r_{1/2} \sim 8 \text{ Mpc}$  by Bajtlik et al. (1988). If we translate this estimate to  $z = 0$  by taking into account the variation of  $J_{\nu_0}^{BCK}(z)$ , we obtain that the Bajtlik et al. local value is  $r_{1/2}^0 \approx \sqrt{40} \times 8 = 50 \text{ Mpc}$  which is sixty times smaller than the value of 3200 Mpc proposed in Table 1. This discrepancy in the values of  $r_{1/2}^0$  (which relates the quasar intensity to the relative strength of  $J_{\nu_0}^{BCK,0}$ ) effectively rules out our simple model.

- **B** – As apparent in Fig. 1, our synthetic ISED rolls down steeply at the lower wavelength limit. If we calculate a similar transmitted ISED but for a reduced range in quasar redshifts (reducing the highest redshift to 1, say), the roll over would be shifted to higher wavelength, a feature not seen in any individual quasar spectrum.
- **C** – The self-imposed requirement that individual absorbers or clumps be of columns  $N_{H^0} \ll 10^{12} \text{ cm}^{-2}$  implies the existence of quite a large number of clumps along the line-of-sight. For a column of  $10^{10} \text{ cm}^{-2}$ , about  $6 \times 10^7$  clumps per unit redshift would be required with an approximate individual mass of about one solar masses (assuming a neutral hydrogen fraction of  $10^{-3}$  and a clump hydrogen density of order  $2 \times 10^{-4}/\text{cc}$ ).

In the case of point C, the number of clumps and their masses is not an unsurmountable objection, however, given the level of speculation characterizing current ideas about the nature of the dark matter. Point B above can also be resolved by having the proposed absorption component disappear at current Epoch (as a result of Compton heating to  $T \gg 10^6 \text{ K}$ , say). The strongest objection is given in which definitely rules out the interplay between quasar and IGM photoionization as the correct physical mechanism for causing the smoothing out of the expected sharp break near  $1000\text{\AA}$  (as the one seen in Model II of Fig. 1). The next step might consist in looking for a different distribution of neutral H than that given in Eqn. 2 which was based on photoionization of line-of-sight clumps. However, objections could then arise about justifying the complexity of the function found and its overall plausibility.

**Acknowledgments.** This work was supported by the Mexican science funding agency CONACyT under grant 32139-E and is based on archived data at the Space Telescope Science Institute which is operated by the Association of Universities for Research in Astronomy, Inc., under NASA contract NAS5-26555. We are indebted to W. Zheng for sharing the original data presented in ZKTGD.

## References

- Bajtlik, S., Duncan, R., Ostriker, J. P. 1988, ApJ, 327, 570  
 Davé, R. & Tripp, T. M. 2001, ApJ, 553, 528  
 Haardt, F. & Madau, P. 1996, ApJ, 461, 20  
 Korista, K., Ferland, G., & Baldwin, J. 1997, ApJ, 487, 555  
 Møller, P., & Jakobsen, P. 1990, A&A, 228, 299  
 O'Brien, P. T., Gondhalekar, P. M., & Wilson, R. 1988, MNRAS, 233, 801  
 Shull, J. M., Roberts, D. Giroux, M. L., Penton, S. V., & Fardal, M. A. 1999, AJ, 118, 1450  
 Pen, U.-L. 1999, ApJS, 120, 49  
 Zheng, W., Kriss, G. A., Telfer, R. C., Grimes, J. P., & Davidsen, A. F. 1997, ApJ, 475, 469 (ZKTGD)